

Electrothermal ac electro-osmosis

Zachary R. Gagnon and Hsueh-Chia Chang^{a)}

Center for Microfluidics and Medical Diagnostics, Department of Chemical and Biomolecular Engineering, University of Notre Dame, Notre Dame, Indiana 46556, USA

(Received 21 September 2008; accepted 12 October 2008; published online 13 January 2009)

Two ac polarization mechanisms, charge accumulation due to electrode double layer charging and bulk permittivity/conductivity gradients generated by Joule heating, are combined in the double layer by introducing zwitterions to produce a new ac electrokinetic pump with the largest velocity (>1 mm/s) and flow penetration depth (100 μm) reported for low-conductivity fluids. The large fluid velocity is due to a quartic scaling with respect to voltage, as is true of electrothermal flow, but exhibits a clear maximum at a frequency corresponding to the electrode double layer inverse RC time. © 2009 American Institute of Physics. [DOI: 10.1063/1.3020720]

The ability to direct fluid flow at length scales of the order of tens of microns is an essential requirement in lab-on-a-chip devices. Conventional solutions often involve scaling down peristaltic, diaphragm, or other popular macroscale mechanical pumps to microscale dimensions.¹ Most such pumps contain moving parts, which can lead to clogging and cell lyses, and render them unsuitable for biological applications. Due to such drawbacks, the use of electrokinetic (EK) micropumps with no moving parts to transport and mix fluid has attracted considerable attention.^{2,3} The most popular include dc and ac micropumps. In a dc pump electro-osmotic (EO) flow is induced by an external tangential electric field E_t produced by pair of electrodes placed on the inlet and outlet of a microchannel.² The applied field within the microchannel produces a tangential Maxwell force within the naturally polarized Debye layer on the channel wall, and through viscous dissipation drives a characteristic Smoluchowski slip velocity $U_s = -\varepsilon\zeta E_t/\mu$, where ε , ζ , and μ are the medium dielectric constant, zeta potential, and viscosity, respectively.

A popular alternative to the dc pump is an ac pump, as the resulting acEO flow is driven by microelectrodes that can be embedded within the chip to affect more precise flow control. The ac field across the microelectrodes is sustained at such a high frequency (100–500 kHz) that Faradaic generation of air bubbles and ionic contaminants is avoided even at high voltages. In contrast, dc pumps necessarily involve a charge transfer reaction at the electrode and are not embeddable. That a zero-mean ac field can induce a nonzero time-averaged tangential Maxwell stress along a polarized electrode surface to drive the acEO flow is quite counterintuitive and was only recently understood.³ The electric field induced electrode polarization occurs because the applied field sustains a time-varying charging current within the working electrolyte solution, charging the double layer on the electrode surface much like a capacitor. The accumulation of charge must partially, but not entirely, screen the external electric field such that there is still a tangential component of the electric field on the induced charge layer on each electrode to generate flow. As such, acEO flow has a distinct maximum at a frequency corresponding to the inverse RC time scale for the electrode-electrolyte circuit

(about 100–500 kHz for most conditions) that scales as $(D/\lambda l)$, where D is the ion diffusivity, λ is the Debye layer thickness, and l is the electrode separation.³ Symmetric electrodes then sustain acEO vortices, while nonsymmetric ones with confinement-induced back pressure can produce a net flow that penetrates beyond the electrodes.⁴ The field induced double layer charging by the external current produces an effective ζ potential, which at low frequencies is typically of the order the applied voltage V . Therefore, the characteristic acEO slip velocity scales quadratically with the applied field $U_s \sim \varepsilon V^2/\mu$ and is typically low (<100 $\mu\text{m/s}$).

Electrothermal (ET) flow is a third option to EK induced fluid flow. ET fluid flow arises from the interaction of the external electric field with temperature-induced inhomogeneities in medium conductivity and permittivity due to Joule heating.^{5,6} The resulting gradients induce a space charge accumulation and depletion under an ac field with an accumulated charge density that can be estimated by the usual Maxwell–Wagner-type charge flux balance between Coulomb and dielectric forces, $\rho = [\sigma(\partial\varepsilon/\partial T) - \varepsilon(\partial\sigma/\partial T)]/(\sigma + i\omega\varepsilon)\nabla T \cdot E$. For frequencies much less than the inverse RC charging time of the bulk electrolyte, $\omega \ll \sigma/\varepsilon \sim 10$ MHz, dielectric forces are minimal compared to Coulombic forces. One can see this as at low frequency the charge density expression can be approximated as $\rho = \varepsilon[(1/\varepsilon)(\partial\varepsilon/\partial T) - (1/\sigma)\times(\partial\sigma/\partial T)]\nabla T \cdot E$. For aqueous solutions, $(1/\varepsilon)(\partial\varepsilon/\partial T) = -0.4\%/^\circ\text{C}$ and $(1/\sigma)(\partial\sigma/\partial T) = 2\%/^\circ\text{C}$.⁵ As the maximum frequency used in this work is 1.2 MHz, much less than the inverse RC charge time, charge density accumulation due to thermal gradients in permittivity will be neglected in all subsequent physical analysis.

In order for strong temperature gradients to exist, reported ET pumping has been limited to higher conductivity fluids, typically greater than 1 S/m, where significant power dissipation and Joule heating become feasible.⁶ As the electric field produced by small disjoint microelectrodes is quite high, typically of the order of $E = 10^5$ V m⁻¹ for a potential of 10 V dropped across a 25 μm gap, there is large power density generated in the fluid surrounding the high field edges of the electrodes. The power generation per unit volume is σE^2 , and for a typical medium conductivity of $\sigma_m = 0.1$ S m⁻¹ and field of 10^5 V m⁻¹ the average power dissipation over a typical picoliter volume of fluid is estimated to be approximately 10 mW. Such a large amount of power

^{a)}Electronic mail: hchang@nd.edu.

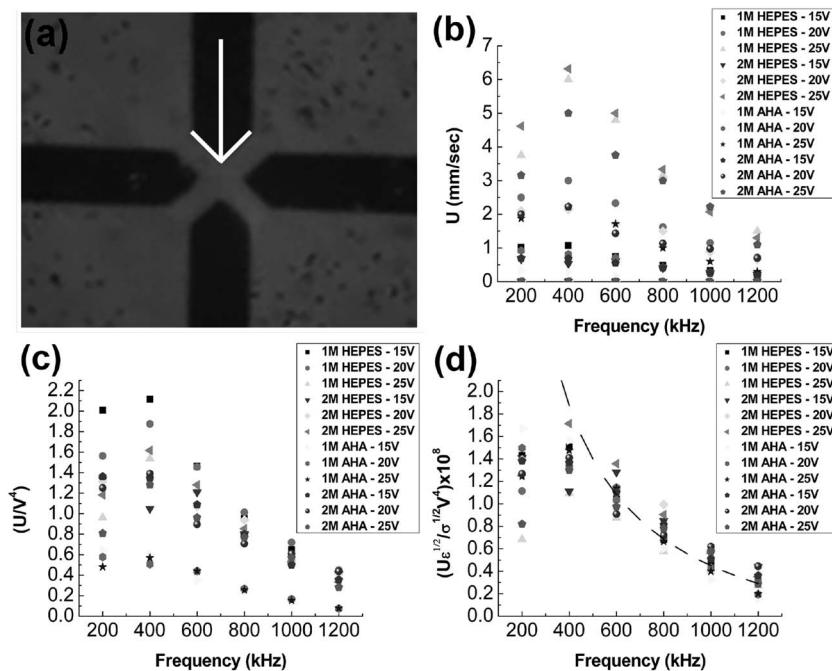


FIG. 1. (a) Fluid pumping over active electrode at 20 V_{p,p}, 400 kHz (Ref. 9). (b) Measured experimental fluid velocity data. (c) Quartic scaled velocity data. (d) Quartic scaling with double layer length scales.

generated in a very small volume can give rise to localized increases in fluid temperature. An order-of-magnitude estimate of this localized temperature increase can be approximated from the steady state energy balance equation as $\Delta T \sim \sigma V^2/k$, where k is the thermal conductivity of the electrolyte. Therefore, one expects temperature-induced space charge density to scale as the cubed power of the applied voltage, resulting in the expected quartic scaling with voltage for the electric body force as $f_E = \rho E \sim E^2 \nabla T \sim E^4$.

Despite a maximum fluid velocity that approaches 1 mm/sec, which due to the quartic scaling is much higher than other EK pumps, ET pumps are still limited to high electrolyte conductivities with large Joule heating. This poses an issue when one wants to integrate other EK phenomena with different electrolyte conductivity specifications, such as dielectrophoresis (DEP), within the same device. DEP has become a very popular means of manipulating particles and cells within microfluidic environments and is the obvious complement to EK pumps for devices that sort, separate, and analyze cells or particles.⁷ Sorting and separation of low-permittivity particles should best be done at low conductivities, such that the particle conductivity is higher than the medium and a crossover frequency exists where separation is most efficient.⁸

In this letter, we extend the use of ET flow to the low-conductivity buffer range that is commonly associated with acEO flow. The approach is to enlarge the double layer thickness with low ionic strength such that a thermal gradient exists in the double layer to enhance the charging rate. A proper screening frequency is then selected such that the field and thermal gradients are confined to the enlarged double layer. As such, charging into the double layer with a thermally induced conductivity gradient combines multiplicatively. We demonstrate that strong ET acEO flow, as great as 6.0 mm/s, can be generated with various types of low-conductivity and biologically compatible zwitterion buffers with low conductivities 100–160 $\mu\text{S}/\text{cm}$, two orders of magnitude less than what has been typically reported,⁸ but high relative dielectric constants between 160–260 to effect a

large double layer charge capacitance. A scaling analysis indicates that the characteristic double layer length scale specific to each electrolyte needs to be included to demonstrate good collapse of the experimental fluid velocity data. These results suggest that the observed fluid motion is not the typical ET flow, but rather an ET enhanced version of acEO flow, thus allowing high-velocity pumping at low conductivities.

A directed flow is generated with an asymmetrically polarized electrode array. As shown from a top view in Fig. 1(a), one of the four electrodes is active, while three others are grounded as such to produce a field focusing effect, and thus a high thermal gradient emanating from the tip of the active electrode. Such asymmetry and the unique polarization mechanisms to be scrutinized produce a net fluid motion down the length of the active electrode. The flow penetration depth of approximately 100 μm beyond the tip is believed to the largest penetration depth reported for EK pumps.⁹

The device was fabricated by patterning dual titanium-gold layers onto precleaned glass slides. Standard 50 \times 75 mm² microscope slides were patterned with the image reversal photoresist Shipley AZ-5214 to define the electrode patterns. Then, 50 \AA of titanium and 2500 \AA of gold were evaporated onto the slides followed by a resist dissolution and metal lift-off in acetone. The array was designed as four triangular posts with an inner square side length of 25 μm and an electrode width of 60 μm . Stock solutions of 1M ($\sigma=157.5 \mu\text{S}/\text{cm}$, $\epsilon_r=170$) and 2M ($\sigma=151.3 \mu\text{S}/\text{cm}$, $\epsilon_r=260$) HEPES, and 1M ($\sigma=118.8 \mu\text{S}/\text{cm}$, $\epsilon_r=160$) and 2M ($\sigma=155.3 \mu\text{S}/\text{cm}$, $\epsilon_r=240$) amino-hexanoic acid (AHA) solution were prepared from reagent grade HEPES (4-(2-hydroxyethyl)-1-piperazineethanesulfonic acid) and AHA obtained from Sigma-Aldrich. Conductivity measurements were measured with a conductivity probe and relative permittivity values were taken from literature.¹⁰ 5 μm polystyrene particles were added to each solution to aid in flow visualization and fluid velocity measurements using a high speed camera (Olympus i-speed) attached to an inverted microscope (Olympus IX71). Each buffer solution was injected

into a cover slip sealed array and the corresponding fluid velocities were measured between 200 and 1200 kHz at 15, 20, and 25 $V_{p.p.}$ over the tip of the active electrode. The resulting data are shown in Fig. 1(b).

The velocity data depict the usual acEO capacitive charging frequency dependence, in that the measured fluid velocity reaches a maximum at intermediate frequencies, signifying the existence of a characteristic RC charging time scale. As ET flow predicts no such maximum, one would expect this behavior to be acEO flow, and the data collapsed with the usual quadratic scaling with applied voltage, $U_s \sim \varepsilon V^2/\mu$.

Interestingly, the data fail to exhibit a quadratic collapse and surprisingly exhibit partial quartic scaling with voltage as shown in Fig. 1(c). Such partial collapse, however, is not indicative of bulk ET flow, as previous work has reported good prediction of ET velocity data with quartic scaling of voltage.⁶

Due to the observed capacitive time scale, incomplete collapse can be attributed to the differing capacitive double layer length scales for each electrolyte used in the experiment. The key is estimating the effective zeta potential ζ of the time-averaged velocity $\varepsilon s E_t/\mu$. As the thermal gradient and charge accumulation occur within the double layer, the proper length scale for charge accumulation is the double layer thickness. Hence, the Poisson equation over a double layer length scale gives $\rho \sim \varepsilon s/\lambda^2$. The effective surface charge density σ_s of the accumulated charges in the double layer is related to the normal electromigration flux into the double layer as a result of the applied field, $i\omega\sigma_s = \sigma \partial\phi/\partial n$. Unlike traditional ET flow with induced space charge in the bulk electrolyte, the accumulated space charge in this work is confined to the double layer, therefore one can approximate the surface charge to space charge density as $\sigma_s \sim \lambda\rho$. The applied potential is dropped across the electrodes of separation L_c , hence $\partial\phi/\partial n \sim V/L_c$. With $\lambda^2 = \varepsilon D/\sigma_0$ the zeta potential can now be expressed as

$$s \sim \frac{\sigma\lambda V}{\omega\varepsilon L_c} \sim \frac{\lambda V\sigma_0}{\omega\varepsilon L_c} \left(\frac{V}{V_0}\right)^2 \sim \frac{DV}{\omega\lambda L_c} \left(\frac{V}{V_0}\right)^2.$$

This scaling includes the linear conductivity variation with respect to the temperature change by Joule heating $\Delta T \sim \sigma_0 V^2/k$, which in turn varies quadratically with respect to the voltage by the ET scaling such that $\sigma = \sigma_0 (V/V_0)^2$, where σ_0 and $V_0 = kT_0/\sigma_0$ are the reference electrolyte conductivity and Joule voltage, respectively.

As the data are taken within an order of magnitude of the frequency corresponding to the inverse RC time with maximum velocity, the tangential electric field is approximately equal to the normal field, and therefore the slip velocity

$$\sim \frac{\varepsilon s E_t}{\mu} \sim \frac{\varepsilon s V}{\mu L_c} \sim \frac{\varepsilon V^2 D}{\omega \mu L_c^2 \lambda} \left(\frac{V}{V_0}\right)^2.$$

Applying a V^4/λ scaling argument to the experimental data, one observes an excellent collapse with a predicted $1/\omega$ scaling with frequency as shown in Fig. 1(d) for all ionic strengths and voltages.

Typically limited to high conductive fluids, such quartic scaling with double layer length scales suggests that field induced Joule heating introduces a conductivity gradient within the electrode double layer to enhance its charge accumulation rate and produce the strong V^4 scaling of the acEO velocity that reaches 6 mm/s even for low-conductivity electrolytes. As Joule heating extends beyond the electrode surface, the directed flow also extends 100 μm beyond the tip of the electrode. ET acEO is hence similar in nature to traditional ET flow; however, it can be easily distinguished from classical bulk ET flow with the presence of a characteristic maximum in measured velocity with respect to the frequency at the inverse charging time of the double layer $\lambda L_c/D$, typically of the order of 100 kHz, followed by a steady decline in measured fluid velocity. Typically, no such maximum exists for classical ET flow and the measured flow direction can actually reverse at high frequencies.⁵ These characteristics make it possible to discriminate ET acEO from the classical case.

¹T. Thorsen, S. J. Maerkl, and S. R. Quake, *Science* **298**, 580 (2002).

²C. H. Chen and J. G. Santiago, *J. Micromech. Microeng.* **11**, 672 (2002).

³A. Gonzalez, A. Ramos, N. G. Green, A. Castellanos, and H. Morgan, *Phys. Rev. E* **61**, 4019 (2000).

⁴A. Ramos, A. Gonzalez, A. Castellanos, N. G. Green, and H. Morgan, *Phys. Rev. E* **67**, 056302 (2003).

⁵A. Ramos, H. Morgon, N. G. Green, and A. Castellanos, *J. Phys. D* **31**, 2338 (1998).

⁶J. Wu, M. Lian, and K. Yang, *Appl. Phys. Lett.* **90**, 234103 (2007).

⁷I. F. Cheng, H. C. Chang, D. Hou, and H.-C. Chang, *Biomicrofluidics* **1**, 021503 (2007).

⁸J. Gordon, Z. Gagnon, and H.-C. Chang, *Biomicrofluidics* **1**, 044102 (2007).

⁹See EPAPS Document No. E-APPLAB-93-022845 for video of directed flow over the activated micropump. For more information on EPAPS, see <http://www.aip.org/pubservs/epaps.html>.

¹⁰W. M. Arnold, *IEEE Trans. Ind. Appl.* **37**, 1468 (2001).